

Quantifying the impact of the Tamm-Dancoff approximation on the computed spectra of transition-metal systems

Muhammed A. Dada,¹ Sarah Pak,¹ Matthew N. Ward,¹ Megan Simons,¹ and Daniel R. Nascimento^{1, a)}
Department of Chemistry, The University of Memphis, Memphis, TN 38152, USA

The Tamm–Dancoff Approximation (TDA) offers a computationally efficient alternative to full linear-response Time-Dependent Density Functional Theory (TDDFT) for calculating electronic excited states, particularly in large molecular systems. By neglecting the coupling between excitation and de-excitation channels, TDA simplifies the TDDFT response equations into a Hermitian form. This not only reduces computational cost but also eliminates numerical instabilities that can arise in the full non-Hermitian formalism. While TDA has been widely explored for valence excitations, its reliability for transition metal complexes and core-level spectroscopies remains largely untested. In this work, we address this gap by systematically comparing TDA and full TDDFT results for a series of transition metal species, focusing on absorption spectra across the UV-Vis, metal K-edges, and L-edges. Our results show that, for core-level excitations, TDA yields excitation energies and oscillator strengths nearly indistinguishable from those obtained with full TDDFT. This agreement is attributed to the negligible contribution of de-excitation amplitudes at high excitation energies, indicating that the omitted coupling terms play an insignificant role in these spectral regimes. These findings validate the accuracy and robustness of TDA in core-level spectra simulations and support its broader application in studies involving transition metal systems.

I. INTRODUCTION

The linear-response formulation of time-dependent density-functional theory (TDDFT) has become a highly popular way to obtain excited-state information of large molecular systems inaccessible to high-accuracy wave-function-based theories. In its standard formulation, given by Casida’s equation, one obtains single-particle density-density polarization amplitudes that can be used to evaluate linear-response properties¹.

It has long been acknowledged that the TDDFT formalism provides significant improvements over simple configuration-interaction singles (CIS) or time-dependent Hartree–Fock (TDHF) treatments, especially in the description of low-lying excited states^{2–6}, and strongly bound excitons⁷. Nonetheless, the coupling between excitation and de-excitation channels present in TDDFT can lead to significant problems in systems that exhibit triplet instabilities⁸. By electing to neglect these interactions — the Tamm-Dancoff Approximation (TDA)⁹ — these problems are eliminated and significant computational savings can be achieved, often with improved results^{10–12}. Since the TDA equations share similarities with the configuration interaction singles (CIS) method, its application in the calculation of excited-state transition moments^{13–18} and non-adiabatic couplings^{19–23} can be easily justifiable.

A critical aspect of the TDA is that the Thomas–Reiche–Kuhn (TRK) dipole sum rule^{24–26} is no longer expected to hold²⁷, oftentimes leading to inconsistent spectral intensities. Garcia-Alvarez and Gozem recently demonstrated that violation of the TRK sum rule can

yield TDA oscillator strengths that are particularly susceptible to the choice of dipole gauge (length vs. velocity)^{28,29}. These problems can be severe for electronic circular dichroism calculations³⁰. Studies on confined systems able to exhibit mixed excitonic-plasmonic behaviour^{31,32} also highlight limitations of the TDA.

In the context of core-level spectroscopies, the TDA is routinely employed without significant scrutiny, as it consistently yields reliable relative excitation energies and oscillator strengths. It is generally accepted that the limitations of TDA observed at low excitation energies do not necessarily extend to the high-energy regime relevant to X-ray spectroscopy. A recent study by Fransson and Pettersson explored the influence of both the TDA and the Core–Valence Separation (CVS) scheme on the calculation of X-ray absorption and emission spectra³³. Their investigation focused primarily on K-edge transitions in light elements, with selected examples involving sulfur and selenium. They concluded that X-ray absorption spectra (XAS) calculations using the TDA and CVS approximations closely reproduce the results obtained from TDDFT treatments.

In the present work, we extend this analysis to a broader set of transition-metal-containing complexes and spectral regions, providing a systematic assessment of the TDA’s performance across a wide excitation energy range. Our results offer quantitative evidence that the coupling between excitation and de-excitation included in TDDFT diminishes rapidly with increasing excitation energy, becoming effectively negligible in the soft X-ray and higher energy regimes. These findings support and further justify the widespread use of the TDA in core-level spectra calculations.

^{a)} Electronic mail: daniel.nascimento@memphis.edu

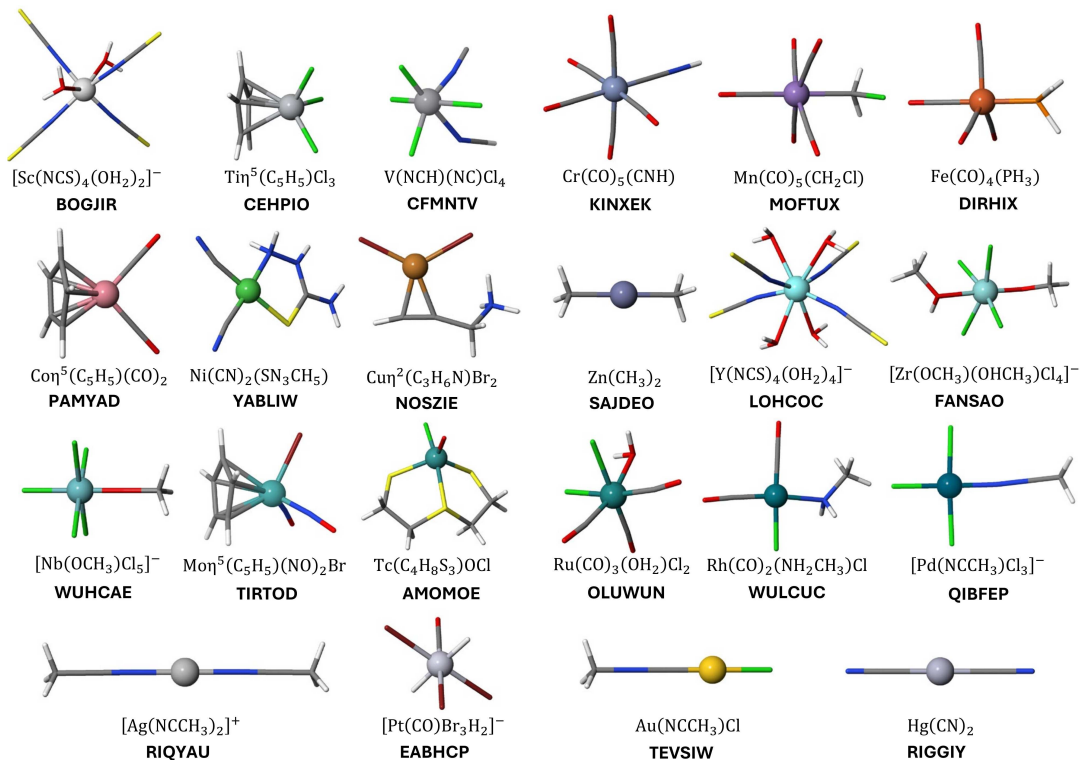


FIG. 1. Collection of 22 transition metal complexes chosen for the present study. Structures were retrieved from the tmQM dataset³⁴ and are shown with their chemical formulas and Cambridge Structural Database (CSD) reference code.

II. METHODOLOGY

The linear-response time-dependent density functional theory problem is given by Casida's equations¹:

$$\begin{pmatrix} \mathbf{A} & \mathbf{B} \\ \mathbf{B} & \mathbf{A} \end{pmatrix} \begin{pmatrix} \mathbf{X} \\ \mathbf{Y} \end{pmatrix} = \Omega \begin{pmatrix} \mathbf{1} & \mathbf{0} \\ \mathbf{0} & -\mathbf{1} \end{pmatrix} \begin{pmatrix} \mathbf{X} \\ \mathbf{Y} \end{pmatrix}, \quad (1)$$

where the elements of the \mathbf{A} and \mathbf{B} matrices are given by

$$A_{ia,jb} = (\epsilon_a - \epsilon_i)\delta_{ij}\delta_{ab} + \frac{\partial F_{ia}}{\partial \rho_{bj}} \quad \text{and} \quad B_{ia,jb} = \frac{\partial F_{ia}}{\partial \rho_{jb}}. \quad (2)$$

Within the standard hybrid adiabatic-local-density approximation (ALDA) formalism³⁵, $\partial F_{ia}/\partial \rho_{jb}$ take the explicit form

$$\frac{\partial F_{ia}}{\partial \rho_{jb}} = \langle ib|aj \rangle - \alpha_{\text{HF}} \langle ib|ja \rangle + f_{ia,bj}^{\text{xc}}, \quad (3)$$

where it is understood that the exchange component of the exchange-correlation response kernel, f^{xc} , has been appropriately scaled by $(1 - \alpha_{\text{HF}})$.

In solving (1), one obtains a pair of solutions corresponding to excitation (X, Y , and Ω) and de-excitation (X^*, Y^* , and $-\Omega$) processes, with the X and Y amplitudes satisfying the condition

$$\langle X^m | X^n \rangle - \langle Y^m | Y^n \rangle = \pm \delta_{mn}, \quad (4)$$

where the positive (negative) sign holds for positive (negative)-frequency solutions.

In the Tamm-Dancoff Approximation, it is assumed that the excitation and de-excitations channels do not couple, and \mathbf{B} is set to zero, leading to a simpler, Hermitian problem

$$\mathbf{A}\mathbf{X} = \Omega\mathbf{X}. \quad (5)$$

Hence, the magnitude of the de-excitation amplitudes vector, \mathbf{Y} , for positive-frequency solutions, is a direct reporter on the extent to which excitation and de-excitations couple via the \mathbf{B} matrix, and thus, on how much TDA and TDDFT are expected to differ.

In this study, we evaluate the squared norm of the de-excitation amplitude vector, $|\mathbf{Y}|^2$, across a range of transition-metal systems and over a broad energy spectrum spanning the UV-Vis region as well as the metal K and L edges. We use this quantity as a metric to assess the expected validity of the Tamm-Dancoff Approximation (TDA). To quantitatively examine discrepancies between TDA and TDDFT, we also analyze several key metrics: spectral area differences, spectral energy shifts, percentage error differences, and R^2 correlation coefficients.

III. COMPUTATIONAL DETAILS

All molecular geometries used in this study (Figure 1) were retrieved from the tmQM dataset³⁴ without further optimization. Ground and excited state calculations were carried out using an in-house code interfaced to PySCF³⁶ and employed three exchange-correlation functionals: B3LYP^{37,38}, PBE0^{39,40}, and PBE⁴¹. A mixed basis set approach was adopted, where the Sapporo-DKH-DZP-2012-diffuse⁴² basis set was used for all transition metal atoms, while the 6-31G*⁴³⁻⁴⁵ Pople basis set was applied to non-metal atoms. Scalar relativistic corrections were incorporated using the Zeroth-Order Regular Approximation (ZORA)⁴⁶⁻⁴⁹.

Core-level absorption spectra were calculated via full diagonalization in the respective K, L₁, L_{2,3}, and UV-Vis subspaces as defined by the core-valence-separation approach⁵⁰. In the UV-Vis case, the occupied space was defined by the a set number of valence orbitals (see supplementary information). A uniform Lorentzian broadening was applied to account for core-hole lifetime effects. The full-width-at-half-maximum (FWHM) for each edge were chosen to be 1.5, 1.0, 0.5, and 0.25 eV for the K, L₁, L_{2,3}, and UV-Vis regions, respectively.

IV. RESULTS AND DISCUSSION

A systematic evaluation of the accuracy of the TDA for the calculation of linear absorption spectra was conducted across a diverse range of transition metal complexes. Since an early study by some of the authors indicates that the exchange-correlation response kernel plays a negligible role in the calculation of core-level spectra⁵¹, we chose to focus our analysis on a single, popular, functional: B3LYP. Nonetheless, our conclusions should be generalizable to any other hybrid GGA functional.

The complexes studied (shown in Figure 1) included all first-row and most second-row transition metals (excluding cadmium due to convergence difficulties), along with prominent third-row representatives: platinum, gold, and mercury.

An initial assessment of the TDA was performed by evaluating $|\mathbf{Y}|^2$ for each excited state in a given spectral region. As indicated in the Theory section, the magnitude of the \mathbf{Y} vector is a direct consequence of the coupling between excitation and de-excitation that are neglected in the TDA. These amplitudes can also be thought of as introducing ground-state correlation^{52,53}.

Figure 2 shows $|\mathbf{Y}|^2$ for all states calculated in a given spectral region (K, L₁, L_{2,3}, or UV-Vis) for all 22 complexes. As one can observe, $|\mathbf{Y}|^2$ is essentially zero for all states above 200 eV and never exceeds 0.07 in the UV-Vis region. The largest concentration of states with $|\mathbf{Y}|^2$ above 0.02 is found at relatively low energies (Fig. 2 inset), indicating that core-level excitations are in essence unaffected by the off-diagonal blocks of the TDDFT response matrix. Based on this information, one can expect

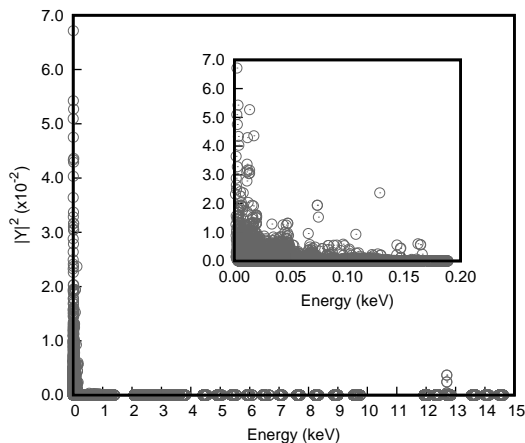


FIG. 2. Magnitude square of the de-excitation amplitudes, \mathbf{Y}^2 as a function of energy covering the 0-15 keV range. The calculated states comprise UV-Vis, metal L, and metal K edges for all 22 complexes. The inset plot highlights the first 200 eV.

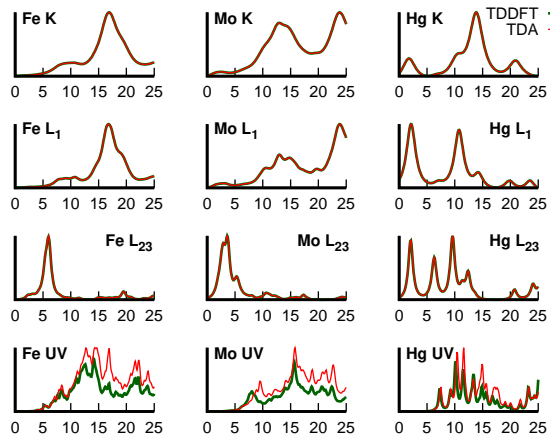


FIG. 3. Calculated UV-Vis, metal K, and metal K spectra for selected complexes with and without the TDA. The plotted spectra shows the first 25 eV near the edge. X-ray plots start at 7,005 eV (Fe K), 822 eV (Fe L₁), 700 eV (Fe L_{2,3}), 19,715 eV (Mo K), 2,800 eV (Mo L₁), 2,517 eV (Mo L_{2,3}), 81,420 eV (Hg K), 14,479 eV (Hg L₁), and 12,692 eV (Hg L_{2,3}).

the TDA and TDDFT methods to yield identical results at sufficiently high energies. Two clear outliers can, however, be observed at about 12.7 keV. The specific data points correspond to the Hg L_{2,3} edge of Hg(CN)₂. In general, we observed that the largest values of $|\mathbf{Y}|^2$ belong to systems containing π -backbonding ligands.

Figure 3 shows the metal K, L₁, and L_{2,3}, and UV-Vis spectra of Fe(CO)₄(PH₃), Mo(C₅H₅)(NO)₂Br, and Hg(CN)₂, identified as some of the species with the largest values of $|\mathbf{Y}|^2$. All the core-level spectra are identical in both TDDFT and TDA cases. Appreciable differences are only visible in the UV-Vis region, where the TDA spectra shows a systematic overestimation of oscillator strengths, consistent with what has been observed

in organic molecules^{28,29}. An important corollary is that deviations from the TRK dipole sum rule resulting from the TDA should be restricted to valence-level excitations.

To better quantify any discrepancies between the two approaches, we evaluate the integrated error over a given spectral region as

$$\Delta I = \int_{E_i}^{E_f} \frac{I_{\text{TDA}}(E) - I_{\text{TDDFT}}(E)}{I_{\text{TDDFT}}(E)} \times 100 dE. \quad (6)$$

This metric provides a direct assessment of the quantitative variations in both the oscillator strengths and excitation energies resulting from the two approaches. The calculated errors are summarized in Figure 4 and Table I.

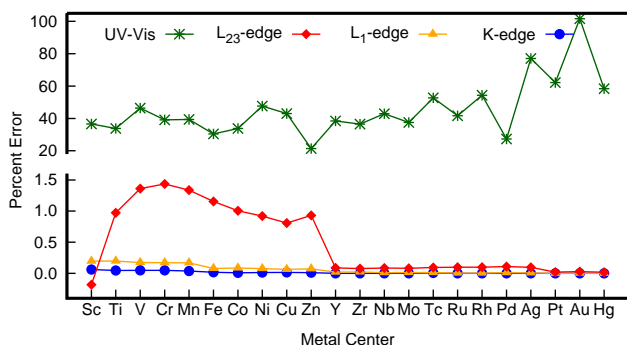


FIG. 4. Percent Error of TDA relative to TDDFT for different spectral regions across the transition metal series.

At the K and L_1 edges, which probe excitations from the $1s$ and $2s$ core orbitals to unoccupied states, respectively, no significant deviations are observed. The errors are at or below 0.2% for all systems. The first-row TMs, show the largest deviations, with percentage errors ranging from 0.06% (Cu) to 0.2% (Sc). Notably, the errors show a slight dependence on the atomic number, with a trend toward smaller discrepancies for heavier elements within this series, resulting from deeper core orbitals. For heavier TMs, the errors are on the order of 0.02% or less.

Larger discrepancies between the TDDFT and TDA spectra become more apparent at the L_{23} edge, which arises from electronic transitions of metal $2p$ core electrons to unoccupied states. Here, there is a clear distinction between the $3d$ and $4d$ complexes. While the $4d$ complexes remain relatively insensitive to the TDA, the $3d$ complexes show significantly larger errors, reaching 1.44% for the chromium complex. Nonetheless, these discrepancies remain small enough to be negligible in any practical application.

The situation is considerably different in the UV-Vis region. In this case, the lowest error was 21% for the zinc complex, which is sufficient to cause qualitative disagreements between the two approaches. One must note, however, that in order to allow full diagonalization, we have restricted valence excitations to a specific set of occupied

Metal	K	L_1	L_{23}	UV-Vis
Sc	0.06	0.20	-0.18	36.54
Ti	0.05	0.20	0.97	33.81
V	0.05	0.17	1.36	46.38
Cr	0.05	0.17	1.44	40.54
Mn	0.04	0.17	1.34	39.36
Fe	0.02	0.08	1.15	41.82
Co	0.01	0.08	1.00	33.79
Ni	0.01	0.08	0.92	47.68
Cu	0.01	0.06	0.81	42.98
Zn	0.01	0.07	0.93	21.34
Y	0.00	0.02	0.09	38.47
Zr	0.00	0.02	0.08	36.49
Nb	0.00	0.01	0.08	42.90
Mo	0.00	0.02	0.09	39.52
Tc	0.01	0.01	0.09	52.74
Ru	0.00	0.00	0.10	41.67
Rh	0.00	0.00	0.10	54.36
Pd	0.00	0.01	0.11	27.32
Ag	0.00	0.01	0.10	77.00
Pt	0.00	0.00	0.02	62.21
Au	0.00	0.00	0.03	90.62
Hg	0.00	0.00	0.02	110.26

TABLE I. Percent Error differences between the TDDFT and TDA spectra for transition metal complexes evaluated at K, L_1 , L_{23} , and UV-Vis spectral regions.

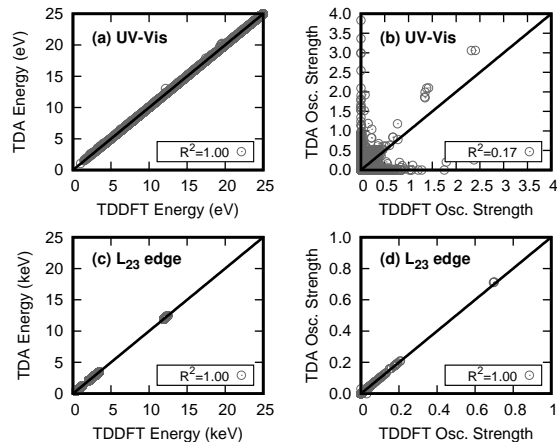


FIG. 5. Correlation plots for excitation energies and oscillator strengths at different spectral regions.

orbitals. We do not expect this restriction to affect our conclusions.

To better assess whether these discrepancies are dominated primarily by errors in the excitation energies or in the oscillator strengths, we generated correlation plots at different energy ranges (Figure. 5).

The TDA and TDDFT energies correlate well in both scenarios, with a linear correlation coefficient R^2 of 1.

While no outliers are observed in the L_{23} or deeper edges, a few outliers can be seen in the UV-Vis case, with a maximum energy deviation of 0.9 eV. Nonetheless, the average error in this region is of only 0.01 ± 0.02 eV. For oscillator strengths, large discrepancies can be observed in the UV-Vis region, with the TDA, in general, severely overestimating TDDFT. Symmetric data points about the diagonal indicate possible changes in the ordering of excited states resulting from qualitative failures of the TDA. Importantly, these problems are not observed at the L_{23} and deeper edges.

V. SUMMARY AND CONCLUSIONS

In summary, we systematically evaluated the accuracy of the Tamm-Dancoff Approximation to TDDFT in the absorption spectra calculation of transition metal complexes across different spectral regions. Our data demonstrated that the de-excitation amplitudes from TDDFT become negligible in the high-energy ($E > 200$ eV) limit, implying that in this regime, TDDFT and TDA yield equivalent spectra. An important consequence of this behavior is that the breakdown of the Thomas-Reiche-Kuhn dipole sum rule, a major disadvantage of the TDA, is restricted to valence-level excitations.

In the UV-Vis region, the TDA results in large errors. These errors are primarily associated with large overestimation of the oscillator strengths, as reported in earlier studies by Garcia-Alvarez and Gozem^{28,29}. Transition metal complexes containing π -backbonding ligands are particularly affected by the couplings between excitation and de-excitation channels in TDDFT, indicating higher levels of excited-state electron correlation in these complexes.

These results further validate and support the use of the TDA in core-level spectra calculations, and reinforce that caution must be taken when employing the TDA in the calculation of UV-Vis spectra, especially if the target excited states exhibit a high-level of electron correlation.

Acknowledgments

This work was supported by the National Science Foundation under the CAREER grant No. CHE-2337902 (M. A. D, S. P, and D. R. N). M. N. W. and M. S. acknowledge support by the University of Memphis. This research also benefited from computational resources provided by the University of Memphis High-Performance Computing Facility.

Data Availability: The data that support the findings of this study are available from the corresponding author upon reasonable request.

¹M. E. Casida and D. Chong, "Recent advances in density functional methods," *Computational Chemistry: Reviews of Current Trends* (1995).

²A. Chantzis, A. D. Laurent, C. Adamo, and D. Jacquemin, "Is the Tamm-Dancoff approximation reliable for the calculation of absorption and fluorescence band shapes?" *Journal of Chemical Theory and Computation* **9**, 4517–4525 (2013).

- ³N. N. Matsuzawa, A. Ishitani, D. A. Dixon, and T. Uda, "Time-dependent density functional theory calculations of photoabsorption spectra in the vacuum ultraviolet region," *Journal of Physical Chemistry A* **105**, 4953–4962 (2001).
- ⁴C. P. Hsu, S. Hirata, and M. Head-Gordon, "Excitation energies from time-dependent density functional theory for linear polyene oligomers: butadiene to decapentaene," *Journal of Physical Chemistry A* **105**, 451–458 (2001).
- ⁵E. S. Kadantsev, M. J. Stott, and A. Rubio, "Electronic structure and excitations in oligoacenes from ab initio calculations," *Journal of Chemical Physics* **124** (2006), 10.1063/1.2186999.
- ⁶R. Gelabert, M. Moreno, and J. M. Lluch, "Charge-transfer $\pi\pi^*$ excited state in the 7-azaindole dimer. A hybrid configuration interactions singles/time-dependent density functional theory description," *Journal of Physical Chemistry A* **110**, 1145–1151 (2006).
- ⁷Y. M. Byun and C. A. Ullrich, "Excitons in solids from time-dependent density-functional theory: Assessing the tamm-dancoff approximation," *Computation* **5** (2017), 10.3390/computation5010009.
- ⁸M. J. Peach, M. J. Williamson, and D. J. Tozer, "Influence of triplet instabilities in TDDFT," *Journal of Chemical Theory and Computation* **7**, 3578–3585 (2011).
- ⁹S. Hirata and M. Head-Gordon, "Time-dependent density functional theory within the tamm-dancoff approximation," *Chem. Phys. Lett.* **314**, 291–299 (1999).
- ¹⁰C. Hu, O. Sugino, and K. Watanabe, "Performance of Tamm-Dancoff approximation on nonadiabatic couplings by time-dependent density functional theory," *Journal of Chemical Physics* **140** (2014), 10.1063/1.4862904.
- ¹¹O. Andreussi, S. Knecht, C. M. Marian, J. Kongsted, and B. Menucci, "Carotenoids and light-harvesting: From DFT/MRCI to the Tamm-Dancoff approximation," *Journal of Chemical Theory and Computation* **11**, 655–666 (2015).
- ¹²T. Rangel, S. M. Hamed, F. Bruneval, and J. B. Neaton, "An assessment of low-lying excitation energies and triplet instabilities of organic molecules with an ab initio Bethe-Salpeter equation approach and the Tamm-Dancoff approximation," *Journal of Chemical Physics* **146** (2017), 10.1063/1.4983126.
- ¹³D. R. Nascimento, E. Biasin, B. I. Poulter, M. Khalil, D. Sokaras, and N. Govind, "Resonant inelastic x-ray scattering calculations of transition metal complexes within a simplified time-dependent density functional theory framework," *J. Chem. Theory Comput.* **17**, 3031–3038 (2021).
- ¹⁴D. R. Nascimento and N. Govind, "Computational approaches for xanes, vtc-xes, and rixs using linear-response time-dependent density functional theory based methods," *Phys. Chem. Chem. Phys.* **24**, 14680–14691 (2022).
- ¹⁵E. Biasin, D. R. Nascimento, B. I. Poulter, B. Abraham, K. Kunnus, A. T. Garcia-Esparza, S. H. Nowak, T. Kroll, R. W. Schoenlein, R. Alonso-Mori, M. Khalil, N. Govind, and D. Sokaras, "Revealing the bonding of solvated ru complexes with valence-to-core resonant inelastic x-ray scattering," *Chem. Sci.* , DOI:10.1039/D0SC06227H (2021).
- ¹⁶F. Segatta, M. Russo, D. R. Nascimento, D. Presti, F. Rigodanza, A. Nenov, A. Bonvicini, A. Arcioni, S. Mukamel, M. Maiuri, L. Muccioli, N. Govind, G. Cerullo, and M. Garavelli, "In Silico Ultrafast Nonlinear Spectroscopy Meets Experiments: The Case of Perylene Bisimide Dye," *Journal of Chemical Theory and Computation* **17**, 7134–7145 (2021).
- ¹⁷S. M. Cavaletto, D. R. Nascimento, Y. Zhang, N. Govind, and S. Mukamel, "Resonant stimulated x-ray raman spectroscopy of mixed-valence manganese complexes," *The Journal of Physical Chemistry Letters* **12**, 5925–5931 (2021).
- ¹⁸B. Gu, S. Cavaletto, D. Nascimento, M. Khalil, N. Govind, and S. Mukamel, "Manipulating valence and core electronic excitations of a transition-metal complex using UV/Vis and X-ray cavities," *Chemical Science* **12** (2021), 10.1039/d1sc01774h.
- ¹⁹Q. Ou, G. D. Bellchambers, F. Furche, and J. E. Subotnik, "First-order derivative couplings between excited states from

- adiabatic tddft response theory,” *J. Chem. Phys.* **142**, 064114 (2015), <https://doi.org/10.1063/1.4906941>.
- ²⁰Q. Ou, E. C. Alguire, and J. E. Subotnik, “Derivative couplings between time-dependent density functional theory excited states in the random-phase approximation based on pseudo-wavefunctions: Behavior around conical intersections,” *J. Phys. Chem. B* **119**, 7150–7161 (2015), <https://doi.org/10.1021/jp5057682>.
- ²¹X. Zhang and J. M. Herbert, “Analytic derivative couplings in time-dependent density functional theory: Quadratic response theory versus pseudo-wavefunction approach,” *J. Chem. Phys.* **142**, 064109 (2015), <https://doi.org/10.1063/1.4907376>.
- ²²E. C. Alguire, Q. Ou, and J. E. Subotnik, “Calculating derivative couplings between time-dependent hartree-fock excited states with pseudo-wavefunctions,” *J. Phys. Chem. B* **119**, 7140–7149 (2015), <https://doi.org/10.1021/jp505767b>.
- ²³X. Sheng, H. Zhu, K. Yin, J. Chen, J. Wang, C. Wang, J. Shao, and F. Chen, “Excited-state absorption by linear response time-dependent density functional theory,” *J. Phys. Chem. C* **124**, 4693–4700 (2020).
- ²⁴W. Thomas, “Über die zahl der dispersionselektronen, die einem stationären zustande zugeordnet sind.(vorläufige mitteilung),” *Naturwissenschaften* **13**, 627–627 (1925).
- ²⁵F. Reiche and W. Thomas, “Über die zahl der dispersionselektronen, die einem stationären zustand zugeordnet sind,” *Zeitschrift für Physik* **34**, 510–525 (1925).
- ²⁶W. Kuhn, “Über die gesamtstärke der von einem zustande ausgehenden absorptionslinien,” *Zeitschrift für Physik* **33**, 408–412 (1925).
- ²⁷A. Dreuw and M. Head-Gordon, “Single-reference ab initio methods for the calculation of excited states of large molecules,” (2005).
- ²⁸J. C. Garcia-Alvarez and S. Gozem, “Absorption Intensities of Organic Molecules from Electronic Structure Calculations versus Experiments: the Effect of Solvation, Method, Basis Set, and Transition Moment Gauge,” *Journal of Chemical Theory and Computation* (2024), [10.1021/acs.jctc.4c00642](https://doi.org/10.1021/acs.jctc.4c00642).
- ²⁹J. C. Garcia-Alvarez and S. Gozem, “Implementation of an Ellipsoidal-Cavity Field Correction for Computed Molecular Oscillator Strengths in Solution: A(nother) Benchmark Study,” *Journal of Chemical Theory and Computation* (2025), [10.1021/acs.jctc.5c00070](https://doi.org/10.1021/acs.jctc.5c00070).
- ³⁰C. Bannwarth and S. Grimme, “Electronic circular dichroism of highly conjugated π -systems: Breakdown of the Tamm-Dancoff/configuration interaction singles approximation,” *Journal of Physical Chemistry A* **119**, 3653–3662 (2015).
- ³¹M. Grüning, A. Marini, and X. Gonze, “Exciton-plasmon states in nanoscale materials: Breakdown of the tamm-dancoff approximation,” *Nano Letters* **9**, 2820–2824 (2009).
- ³²D. Rocca, M. Vörös, A. Gali, and G. Galli, “Ab initio optoelectronic properties of silicon nanoparticles: Excitation energies, sum rules, and Tamm-Dancoff approximation,” *Journal of Chemical Theory and Computation* **10**, 3290–3298 (2014).
- ³³T. Fransson and L. G. Pettersson, “Evaluating the Impact of the Tamm-Dancoff Approximation on X-ray Spectrum Calculations,” *Journal of Chemical Theory and Computation* **20**, 2181–2191 (2024).
- ³⁴D. Balcells and B. B. Skjelstad, “tmqm dataset—quantum geometries and properties of 86k transition metal complexes,” *Journal of Chemical Information and Modeling* **60**, 6135–6146 (2020), PMID: 33166143.
- ³⁵F. Furche and R. Ahlrichs, “Adiabatic time-dependent density functional methods for excited state properties,” *Journal of Chemical Physics* **117**, 7433–7447 (2002).
- ³⁶Q. Sun, T. C. Berkelbach, N. S. Blunt, G. H. Booth, S. Guo, Z. Li, J. Liu, J. D. McClain, E. R. Sayfutyarova, S. Sharma, S. Wouters, and G. K.-L. Chan, “Pyscf: the python-based simulations of chemistry framework,” *Wiley Interdiscip. Rev. Comput. Mol. Sci.* **8**, e1340 (2018), <https://wires.onlinelibrary.wiley.com/doi/pdf/10.1002/wcms.1340>.
- ³⁷A. D. Becke, “Density-functional exchange-energy approximation with correct asymptotic behavior,” *Phys. Rev. A* **38**, 3098–3100 (1988).
- ³⁸C. Lee, W. Yang, and R. G. Parr, “Development of the colle-salvetti correlation-energy formula into a functional of the electron density,” *Phys. Rev. B* **37**, 785–789 (1988).
- ³⁹J. P. Perdew, M. Ernzerhof, and K. Burke, “Rationale for mixing exact exchange with density functional approximations,” *J. Chem. Phys.* **105**, 9982–9985 (1996).
- ⁴⁰C. Adamo and V. Barone, “Toward reliable density functional methods without adjustable parameters: The pbe0 model,” *J. Chem. Phys.* **110**, 6158–6170 (1999).
- ⁴¹J. P. Perdew, K. Burke, and M. Ernzerhof, “Generalized gradient approximation made simple,” *Phys. Rev. Lett.* **77**, 3865–3868 (1996).
- ⁴²T. Noro, M. Sekiya, and T. Koga, “Segmented contracted basis sets for atoms h through xe: Sapporo-(dk)-nzp sets ($n = d, t, q$),” *Theor. Chem. Acc.* **131**, 1124 (2012).
- ⁴³R. Ditchfield, W. J. Hehre, and J. A. Pople, “Self-consistent molecular-orbital methods. ix. an extended gaussian-type basis for molecular-orbital studies of organic molecules,” *J. Chem. Phys.* **54**, 724–728 (1971).
- ⁴⁴W. J. Hehre, R. Ditchfield, and J. A. Pople, “Self-consistent molecular orbital methods. xii. further extensions of gaussian-type basis sets for use in molecular orbital studies of organic molecules,” *J. Chem. Phys.* **56**, 2257–2261 (1972).
- ⁴⁵P. C. Hariharan and J. A. Pople, “The influence of polarization functions on molecular orbital hydrogenation energies,” *Theor. Chim. Acta* **28**, 213–222 (1973).
- ⁴⁶E. van Lenthe, E. J. Baerends, and J. G. Snijders, “Relativistic total energy using regular approximations,” *J. Chem. Phys.* **101**, 9783–9792 (1994), <https://doi.org/10.1063/1.467943>.
- ⁴⁷C. van Wüllen, “Molecular density functional calculations in the regular relativistic approximation: Method, application to coinage metal diatomics, hydrides, fluorides and chlorides, and comparison with first-order relativistic calculations,” *J. Chem. Phys.* **109**, 392–399 (1998).
- ⁴⁸P. Nichols, N. Govind, E. J. Bylaska, and W. A. de Jong, “Gaussian Basis Set and Planewave Relativistic Spin-Orbit Methods in NWChem,” *J. Chem. Theory Comput.* **5**, 491–499 (2009).
- ⁴⁹S. Pak, M. A. Dada, N. Govind, and D. R. Nascimento, “Fast simulation of soft x-ray near-edge spectra using a relativistic state-interaction approach: Application to closed-shell transition metal complexes,” *arXiv preprint arXiv:2503.15462* (2025).
- ⁵⁰L. S. Cederbaum, W. Domcke, and J. Schirmer, “Many-body theory of core holes,” *Phys. Rev. A* **22**, 206 (1980).
- ⁵¹S. Pak and D. R. Nascimento, “The role of the coupling matrix elements in time-dependent density functional theory on the simulation of core-level spectra of transition metal complexes,” *Electron. Struct.* **6**, 015014 (2024).
- ⁵²D. Rowe, “Equations-of-motion method and the extended shell model,” *Reviews of Modern Physics* **40**, 153 (1968).
- ⁵³G. E. Scuseria, T. M. Henderson, and D. C. Sorensen, “The ground state correlation energy of the random phase approximation from a ring coupled cluster doubles approach,” *The Journal of Chemical Physics* **129**, 231101 (2008), https://pubs.aip.org/aip/jcp/article-pdf/doi/10.1063/1.3043729/16660454/231101_1_online.pdf.

Supplementary Information: Quantifying the impact of the Tamm-Dancoff approximation on the computed spectra of transition-metal systems

Muhammed A. Dada,¹ Sarah Pak,¹ Matthew N. Ward,¹ Megan Simons,¹ and Daniel R. Nascimento^{1, a)}

Department of Chemistry, The University of Memphis, Memphis, TN 38152, USA

^{a)}Electronic mail: daniel.nascimento@memphis.edu

I. ACTIVE OCCUPIED MOLECULAR ORBITALS DEFINING THE CORE-VALENCE SEPARATION

CSD Reference Code	Metal	K	L ₁	L ₂₃	UV-Vis
BOGJIR	Sc	1	8	9–11	72–79
CEHPIO	Ti	1	5	6–8	39–54
CFMNTV	V	1	6	7–9	41–59
KINXEK	Cr	1	2	3–5	27–54
MOFTUX	Mn	1	3	4–6	32–60
DIRHIX	Fe	1	3	4–6	27–50
PAMYAD	Co	1	2	3–5	40–45
YABLIW	Ni	1	3	4–6	34–51
NOSZIE	Cu	3	12	13–15	53–65
SAJDEO	Zn	1	2	3–5	19–24
LOHCOC	Y	1	6	7–9	91–98
FANSAO	Zr	1	6	7–9	51–72
WUHCAE	Nb	1	7	8–10	56–72
TIRTOD	Mo	1	3	4–6	50–71
AMOMOE	Tc	1	2	4–6	53–74
OLUWUN	Ru	1	2	3–5	42–65
WULCUC	Rh	1	2	3–5	35–54
QIBFEP	Pd	1	2	3–5	55–60
RIQYAU	Ag	1	2	3–5	29–45
EABHCP	Pt	1	2	6–8	83–100
TEVSIW	Au	1	2	3–5	44–59
RIGGIY	Hg	1	2	3–5	39–53

TABLE I. the range of orbitals chosen for the calculation.

II. ERROR METRICS FOR THE PBE AND PBE0 FUNCTIONALS

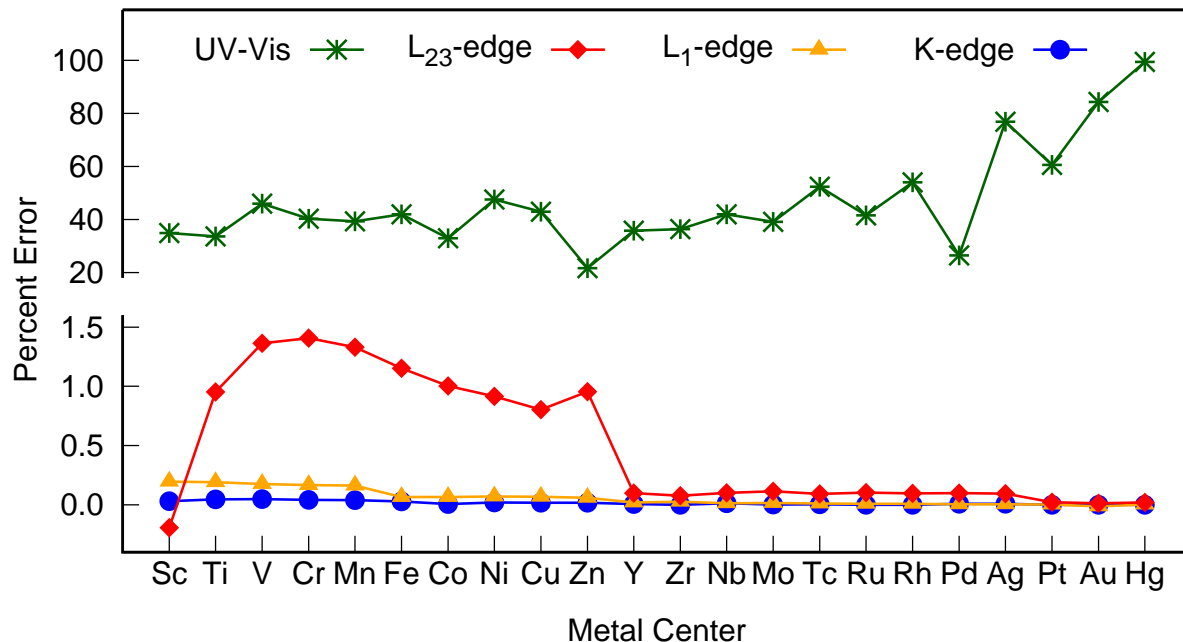


FIG. 1. Percent Error of TDA relative to TDDFT for different spectral regions across the transition metal series obtained with the PBE0 functional.

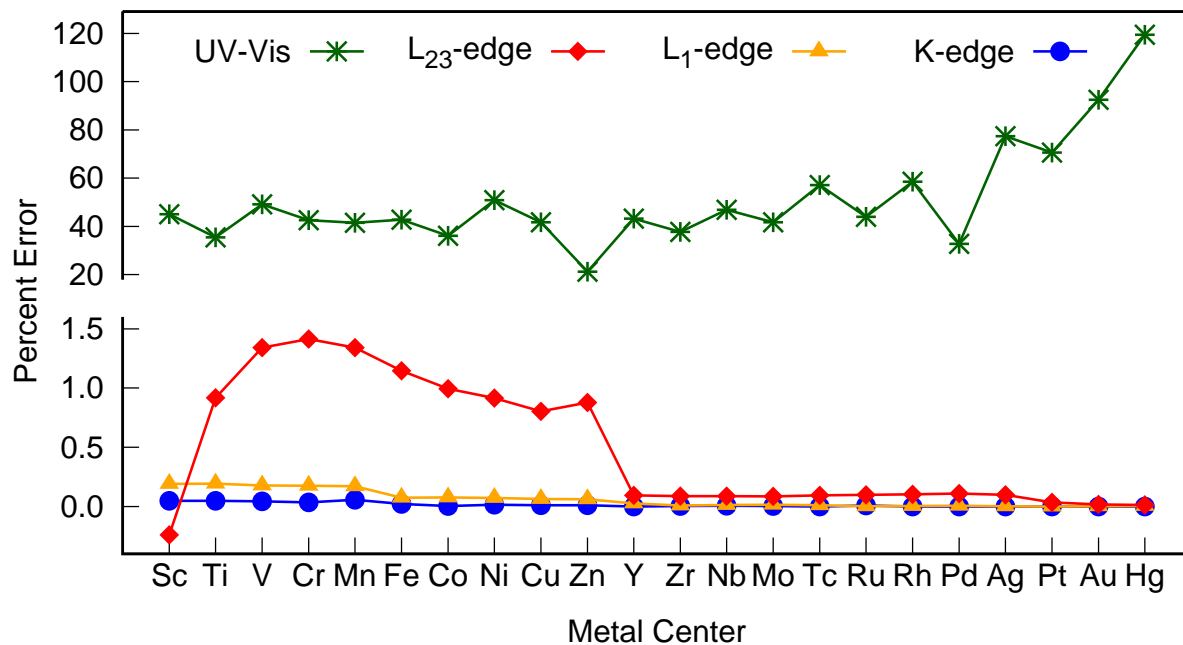


FIG. 2. Percent Error of TDA relative to TDDFT for different spectral regions across the transition metal series obtained with the PBE functional.

Metal	K	L ₁	L ₂₃	UV-Vis
Sc	0.03	0.19	-0.19	34.86
Ti	0.05	0.19	0.95	33.63
V	0.05	0.18	1.36	45.95
Cr	0.04	0.17	1.41	40.28
Mn	0.04	0.16	1.33	39.25
Fe	0.03	0.07	1.15	41.95
Co	0.01	0.07	1.00	32.94
Ni	0.02	0.07	0.92	47.49
Cu	0.02	0.07	0.80	42.90
Zn	0.02	0.06	0.96	21.62
Y	0.01	0.02	0.10	35.78
Zr	0.00	0.02	0.08	36.32
Nb	0.01	0.01	0.10	41.93
Mo	0.00	0.02	0.11	39.11
Tc	0.00	0.01	0.09	52.31
Ru	0.00	0.01	0.10	41.49
Rh	0.00	0.01	0.10	53.96
Pd	0.01	0.00	0.10	26.47
Ag	0.01	0.00	0.09	76.85
Pt	0.00	0.00	0.02	60.52
Au	0.00	-0.01	0.01	84.26
Hg	0.00	0.00	0.02	99.40

TABLE II. Percent error differences between the TDDFT and TDA spectra for transition-metal complexes evaluated at K, L₁, L₂₃, and UV-Vis spectral regions obtained with the PBE0 functional.

Metal	K	L₁	L₂₃	UV-Vis
Sc	0.05	0.19	-0.24	45.08
Ti	0.05	0.19	0.92	35.45
V	0.04	0.18	1.34	49.14
Cr	0.03	0.18	1.41	42.59
Mn	0.06	0.17	1.34	41.49
Fe	0.02	0.07	1.15	42.80
Co	0.00	0.08	0.99	36.12
Ni	0.02	0.07	0.92	50.83
Cu	0.01	0.06	0.80	41.73
Zn	0.01	0.06	0.88	21.21
Y	0.00	0.03	0.09	43.24
Zr	0.00	0.01	0.09	37.74
Nb	0.01	0.01	0.09	46.88
Mo	0.00	0.01	0.08	41.68
Tc	0.00	0.01	0.09	57.08
Ru	0.01	0.00	0.10	43.98
Rh	0.00	0.00	0.10	58.54
Pd	0.00	0.01	0.11	32.72
Ag	0.00	0.00	0.10	77.42
Pt	0.00	0.00	0.03	70.63
Au	0.00	0.00	0.02	92.52
Hg	0.00	0.00	0.01	119.40

TABLE III. Percent error differences between the TDDFT and TDA spectra for transition-metal complexes evaluated at K, L₁, L₂₃, and UV-Vis spectral regions obtained with the PBE functional.